

Current source density reconstruction from incomplete data

Daniel K. Wójcik, Szymon Łęski

Department of Neurophysiology,
Nencki Institute of Experimental Biology,
3 Pasteur Street, 02-093 Warsaw, Poland

April 5, 2009

We propose two ways of estimating the current source density (CSD) from measurements of voltage on a Cartesian grid with missing recording points using the inverse CSD method. The simplest approach is to substitute local averages (LA) in place of missing data. A more elaborate alternative is to estimate a smaller number of CSD parameters than the actual number of recordings and to take the least-squares fit (LS). We compare the two approaches in the three dimensional case on several sets of surrogate and experimental data, for varying numbers of missing data points, and discuss their advantages and drawbacks. One can construct CSD distributions for which one or the other approach is better. However, in general, LA method is to be recommended being more stable and more robust to variations in the recorded fields.

1 Introduction

A common measure of neural population activity is the local field potential (LFP), the low-frequency part of the extracellular electric potential (Nunez & Srinivasan 2005). The LFP is generated by trans-membrane currents in neighboring cells which are usually described on a coarse-grained level by the current source density (CSD) (Plonsey 1969, Nicholson & Freeman 1975, Freeman & Nicholson 1975, Mitzdorf 1985, Nunez & Srinivasan 2005). In the quasi-static approximation the relation of the CSD, C , to the potentials, ϕ , is

$$\nabla(\sigma\nabla\phi) = -C, \quad (1)$$

where σ is the electrical conductivity tensor. For simplicity we assume σ to be a constant scalar (isotropic, homogeneous medium), although in general this condition needs not hold, or even the assumption of purely resistive medium may not be valid (Holsheimer 1987, Ibarz et al. 2006, Logothetis et al. 2007, Makarova et al. 2008). One consequence of Eq. (1)

is non-locality: ϕ is not trivial even in regions where $C = 0$. This means that the recorded LFP may reflect the activity of quite distant cells.

When the recordings of LFP at several locations are available one can attempt reconstruction of the CSD which generated them (Nicholson & Freeman 1975, Freeman & Nicholson 1975, Mitzdorf 1985). Such recordings can be obtained e. g. with an electrode with multiple contacts or with a two-dimensional multi-electrode array (Csicsvari et al. 2003, Barthó et al. 2004, Buzsáki 2004).

The simplest method to calculate CSD is to use a numerical approximation of the second derivative of the potential (Nicholson & Freeman 1975, Freeman & Nicholson 1975, Mitzdorf 1985), e. g. in case of 1-D electrode with equidistant contact points spaced by h one obtains (for interior contacts):

$$C(z_i) = -\sigma \frac{\phi(z_i + h) - 2\phi(z_i) + \phi(z_i - h)}{h^2}. \quad (2)$$

This approach has been extensively used to obtain and analyse CSD in a variety of experimental situations, for example in visual (Rajkai et al. 2008), somatosensory (Lipton et al. 2006), and auditory (Lakatos et al. 2005) cortices of macaque, in subcortical structures (Schroeder et al. 1992), in cerebellum (de Solages et al. 2008), in hippocampus (Ylinen et al. 1995) and in hippocampal slices (Shimono et al. 2000). However, such an approach has certain disadvantages. One of them is that Eq. (2) cannot be applied to boundary points. This is particularly inconvenient in case of two- or three-dimensional data, where the boundary may comprise majority of the points (Łęski et al. 2007).

Another method for estimating the CSD is the inverse CSD (iCSD) method (Pettersen et al. 2006, Łęski et al. 2007). Here one does not try to use Eq. (1) directly (which is the case in traditional CSD). Instead, the idea is to establish a one-to-one relation F between measured voltages and CSD distributions *via* inversion of the forward solution. This is achieved in the following way: assume N recording points on a Cartesian grid (one-, two- or three-dimensional). Consider N -parameter family of CSD distributions — this means that given the values of the N parameters one can assign a value of CSD to each spatial position. Then the values of the potential, ϕ , on the grid can be obtained by solving a well-posed boundary value problem related to the elliptic partial differential equation, Eq. (1) (forward solution). Therefore, the N measured voltages are functions of the CSD parameters. If the family and the parameterization are chosen well, one can invert this relation and from the N measured potentials recover the N parameters of CSD. Usually one parameterizes the CSD with its values on the measurement grid and interpolates between the grid points, linearly or with splines, but there are more possibilities (Pettersen et al. 2006, Łęski et al. 2007).

The aim of the inverse current source density method is to reconstruct the CSD within the volume spanned by the recording grid. Therefore, it seems natural to use in this scheme a family of CSD distributions for which the CSD is non-zero only inside the grid. However, it appears that such a choice may lead to large reconstruction errors (Łęski et al. 2007). This is because usually the actual CSD extends in the tissue beyond the grid set by the measurement points and the sources located just outside the grid may lead to artifacts in the reconstructed density. One way to reduce these errors is to consider a family of CSD distributions extending one layer beyond the original grid. One can set the CSD values at the additional nodes to zero or duplicate the value from the neighboring node of the original grid. In (Łęski et al. 2007) these two approaches were denoted by B or D boundary conditions, respectively, and it was shown that they improve the reconstruction

quality *within the grid*. Note that the extended CSD family is still parameterized with its N values at the original grid and that the intention of such a procedure is to improve the reconstruction fidelity inside the grid and not to estimate the CSD outside.

2 Inverse CSD on incomplete data

A practical problem in the application of the iCSD method to real datasets is how to deal with missing recording points. Such cases arise surprisingly often in real experiments. There may be several reasons for this: a contact of a multi-electrode may not be functioning, some channels may be used for other purposes (e. g. stimulation), or the experiment may be terminated early before all the data are collected.

One way to deal with such data is to patch them with the mean of the neighboring potentials of a missing contact (Łęski et al. 2008). We denote this method by LA for local averages. This approach means replacing the missing true potential at a point with a linear approximation estimated from the neighbors. A more elaborate alternative is to reduce the size of the CSD grid and find the least-squares solution to such an overdetermined system. That means choosing such values of the parameters of the CSD spanned on a smaller grid which minimize the sum of squared differences in potential at all the available electrode points. We denote this method by LS for least squares. The advantage of this approach is that we use only the available data without making any assumptions about the missing recordings, so it seems to be better motivated than LA. However, we decrease the spatial resolution of the reconstructed CSD so it is hard to tell *a priori* which approach is better.

3 Gaussian sources

To compare the quality of the two solutions we first tested them both on three-dimensional surrogate Gaussian sources (Fig. 1). We calculated the potentials on a grid of $(x, y, z) \in 4 \times 10 \times 4$ equally spaced points. Details of the structure of the sources and calculation of LFP are given in the Appendix. This choice of the sources and the grid was motivated by an experimental study of evoked potentials in the barrel cortex of the rat¹. The Gaussian sources represent localized areas of transmembrane currents. The sources were elongated along the y axes so that the conclusions would hold for cortical dipoles generated by active pyramidal cells. We chose this model for its simplicity, as our focus was on testing properties of the methods. The applicability of this model is limited, as it is unlikely that it would approximate the real sources in the cerebral cortex at fine spatial scales. Therefore we do not make any statements about the actual cortical fields. For that purpose one should use much more sophisticated models, for example dipole generators (Tenke et al. 1993). One could also couple cortical dynamics calculated in a neural-mass model with LFP templates obtained from a detailed compartmental model of a pyramidal cell (Pettersen et al. 2008).

For the tests we removed a number of virtual ‘recording points’, reconstructed the CSD using both LA and LS methods, and compared the normalized L^2 reconstruction errors (Łęski et al. 2007): $e = \int (C - \hat{C})^2 dx / \int C^2 dx$, where C is the original and \hat{C} is the reconstructed CSD. For the LS method we used a grid of $4 \times 8 \times 4$ points which covered the whole space occupied by the original grid. This implied larger spacing in the y direction. The iCSD reconstruction was performed with the MATLAB scripts from

¹J. Kamiński, private communication

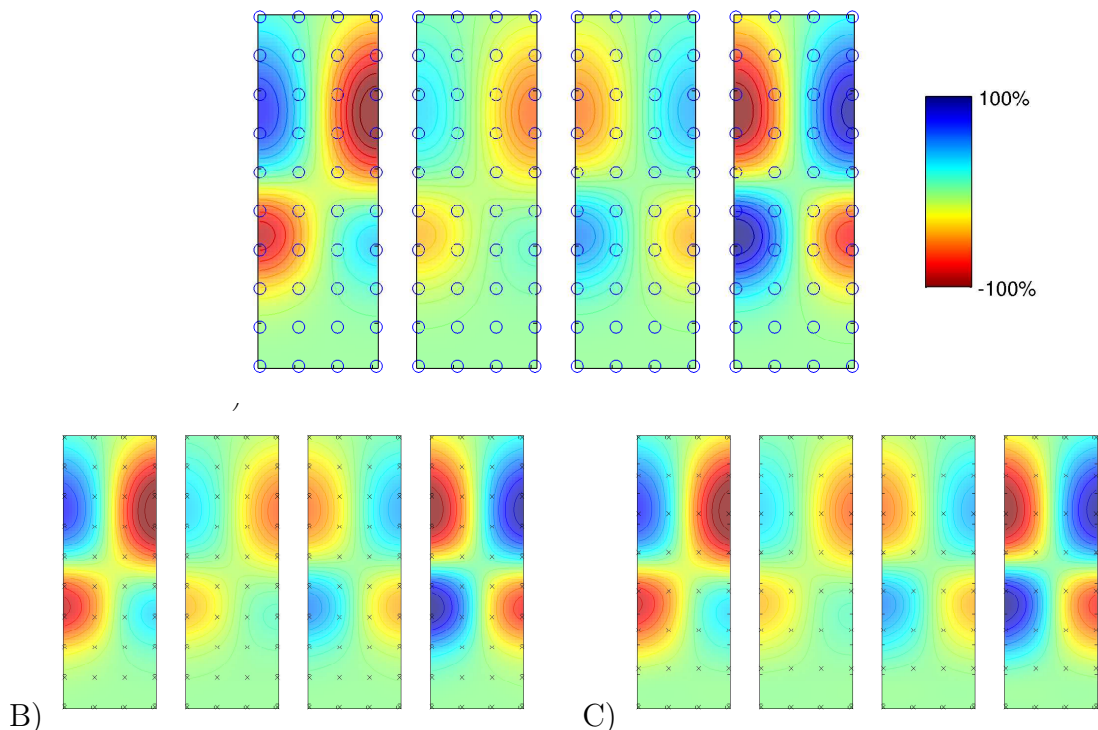


Figure 1: A) Gaussian sources studied in Section 3, four consecutive slices ($x = 1 \dots 4$) through the volume. Electrode positions are marked with circles. B) Reconstruction of the CSD distribution spanned on the full $4 \times 10 \times 4$ grid from the set of potentials calculated at the nodes of the grid (denoted by x's). C) Reconstruction using LS method on complete data; spanned on a smaller, $4 \times 8 \times 4$ grid.

Łęski et al. (2007), modified for the situation at hand. We used not-a-knot splines with D boundary conditions.²

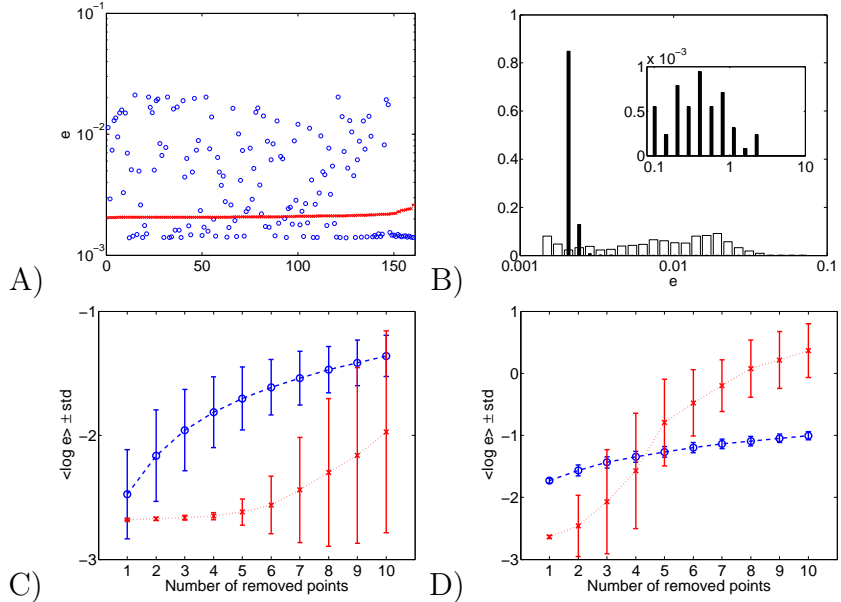


Figure 2: Comparison of local averages (LA) and least squares (LS) methods of reconstructing CSD from incomplete data. A) Results of reconstruction in the case of a single recording point removed from the grid. Normalized reconstruction error for all 160 possibilities, LS: x's, LA: o's, sorted according to the LS error. B) Histogram of normalized reconstruction errors for a pair of grid points removed. Thick bars: LA, thin bars: LS. Inset: outliers in the LS method. C) Comparison of LA (o's) and LS (x's) methods for varying number n of recording points removed from the grid (X axis). Y axis: average logarithm of normalized reconstruction error, error bars are \pm standard deviation, for the best 90% out of 2000 random choices of removed points (except $n = 1$ where 90% of all 160 possibilities are taken). D) Same as C, but for the worst 10% of the cases.

Standard iCSD reconstruction from the calculated potentials gives reconstruction error e of 0.14%. This indicates the quality of the reconstructed approximation of the smooth Gaussian sources by a set of splines spanned on the grid of recorded points. The LS method applied for the reduced grid gives $e = 0.21\%$ which shows how little information is lost when the number of nodes of the grid used for the reconstruction is reduced by 20%, see Figure 1. This is possible in this case thanks to the relatively large extent and slow variation of the sources in the y direction: the sparser grid is still dense enough to effectively sample the sources. In general, the degradation of the reconstruction quality caused by using a sparser grid will strongly depend on how rapidly the CSD varies in space, see Section 4.

We have scanned all the 160 cases of one recording point withdrawn. The LS method gives stable reconstruction error from $e = 0.21\%$ to $e = 0.26\%$. The error of the LA method ranges from $e = 0.14\%$ (which means that the missing datum was indeed the mean of its neighbors) up to 2.1%, see Fig. 2A.

²By D boundary conditions we mean solution on a larger grid with one extra layer added in every direction beyond the original. We assume identical CSD at the added layer and its nearest neighbor in the original grid. ‘Not-a-knot’ splines are the cubic splines implemented in MATLAB, they differ from ‘normal’ splines in the conditions at the extreme points. See Łęski et al. (2007) for details.

There are 12720 possible choices of a pair of electrodes for the set of recording points considered. Here the results are more intricate: as before, LS typically gives smaller errors (Fig. 2B), but from time to time a huge error occurs, with e reaching 270% (63 outliers shown in an inset in Fig. 2B). The outliers can occur only for specific configuration of the missing pair (x_1, y_1, z_1) , (x_2, y_2, z_2) . The necessary (but not sufficient) conditions for large errors are $(x_1, z_1) = (x_2, z_2)$ and $(y_1, y_2) \in \{(1, 2), (1, 3), (2, 3), (9, 10), (8, 10), (8, 9)\}$. There are only 96 of such troublesome pairs and all the outliers in Fig. 2B are of this type.

With growing number of missing recording points the reconstructions become less and less reliable with the LS method becoming monotonically worse with respect to the LA method, Fig. 2C, D. Interestingly, the distributions of the results qualitatively have the same character as in the case of two missing electrodes: that is, the errors of LA method have a unimodal distribution while the distributions of errors in the LS approach have two modes, one with results better than for LA, the other with extremely large errors. The mean error of the LA method also grows but huge errors do not occur. Figures 2C, D show the results obtained for 2000 random choices of the missing recording points.

4 Experimental data

The second part of the test of the two methods was performed on three-dimensional recordings in the rat forebrain of potentials evoked by the deflection of a bunch of whiskers (Łęski et al. 2007). The recordings were made on a grid of $4 \times 5 \times 7$ points. Here we analyse the same two representative latencies which were used as illustrations in Łęski et al. (2007), where the dataset is described in detail.

We perform the same analysis as for the Gaussian sources, apart from the fact that now we do not know the real CSD. Therefore, as the reference C we take the reconstruction spanned on the full $4 \times 5 \times 7$ grid calculated from the full set of recordings. Such C is the best representation of real CSD in the tissue available to us.

Figure 3A shows the reference data set and Fig. 3B shows the CSD reconstructed by LS method on a sparser, $4 \times 5 \times 6$ grid, from the complete set of recorded potentials, 3.5ms after the stimulus onset. Already here we can observe how the intricate structure of activation in the tissue is distorted ($e = 21\%$) when using a smaller spanning grid which was not the case for the Gaussian sources modeling the cortical CSD (Sec. 3).

Clearly, performing reconstructions from incomplete data, we expect the distortions to grow. Results of the test of the two methods are shown in Fig. 4. Fig. 4A shows the results of the iCSD reconstructions from data with one electrode removed. As in the previous case, the distribution of errors of the LS method is bimodal with very narrow modes, while the distribution of errors of the LA method is rather broad (Fig. 4B). However, unlike the previous case, the LA method is almost always better. This difference is preserved as the number of removed points is increased. For both methods the mean error of reconstruction grows with the number of removed points, which is expected. However, the distribution of errors for the LS methods gets wider, while the distribution of errors for LA method gets more narrow. This is true for both the best 90% cases and for the 10% worst. In practice this means that the LS method for such complicated CSD distributions is not recommended.

Such behavior was typical for this data set for the time frames we inspected. For illustration and comparison we show the reconstructions from the complete data on the original (Fig. 5A) and smaller (Fig. 5B) grids as well as the results of the same analysis for the recordings taken 15ms after the stimulus onset (Fig. 6).

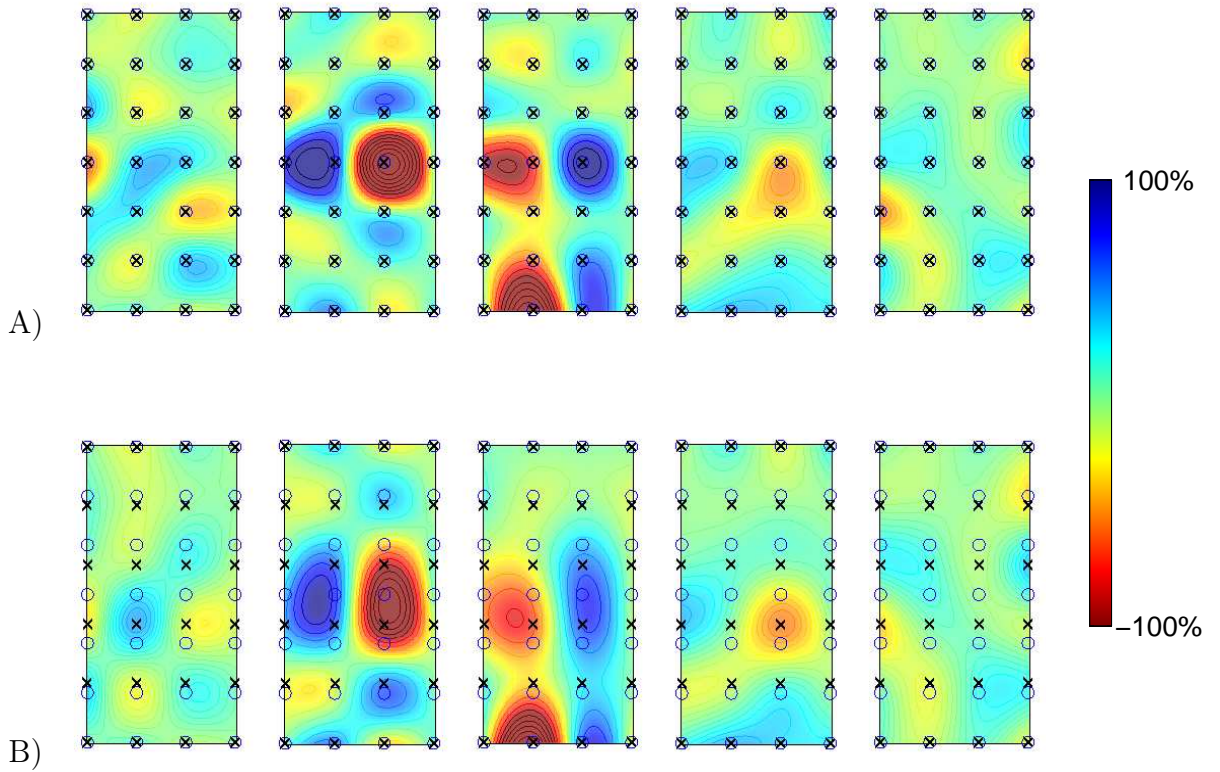


Figure 3: Reconstructions of CSD from experimental data, $t = 3.5\text{ms}$ after stimulation of vibrissa. Each row presents a three-dimensional region of the rat forebrain. The electrode positions ($4 \times 5 \times 7$ grid) are marked with circles, nodes of the grid are marked with x's. A) The reference data set: CSD reconstructed on the full electrode grid. B) CSD reconstructed from the complete set of recordings but spanned on a sparser $4 \times 5 \times 6$ grid. Note that some sources are not adequately sampled using the sparser grid.

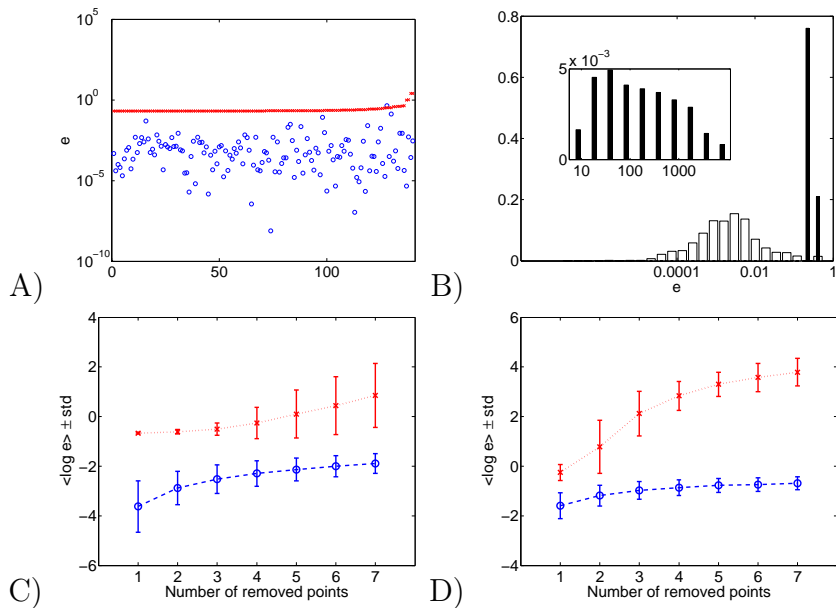


Figure 4: Comparison of LA and LS methods of reconstructing CSD from incomplete data, see caption of Figure 2. The data used here are the same as in Figure 3.

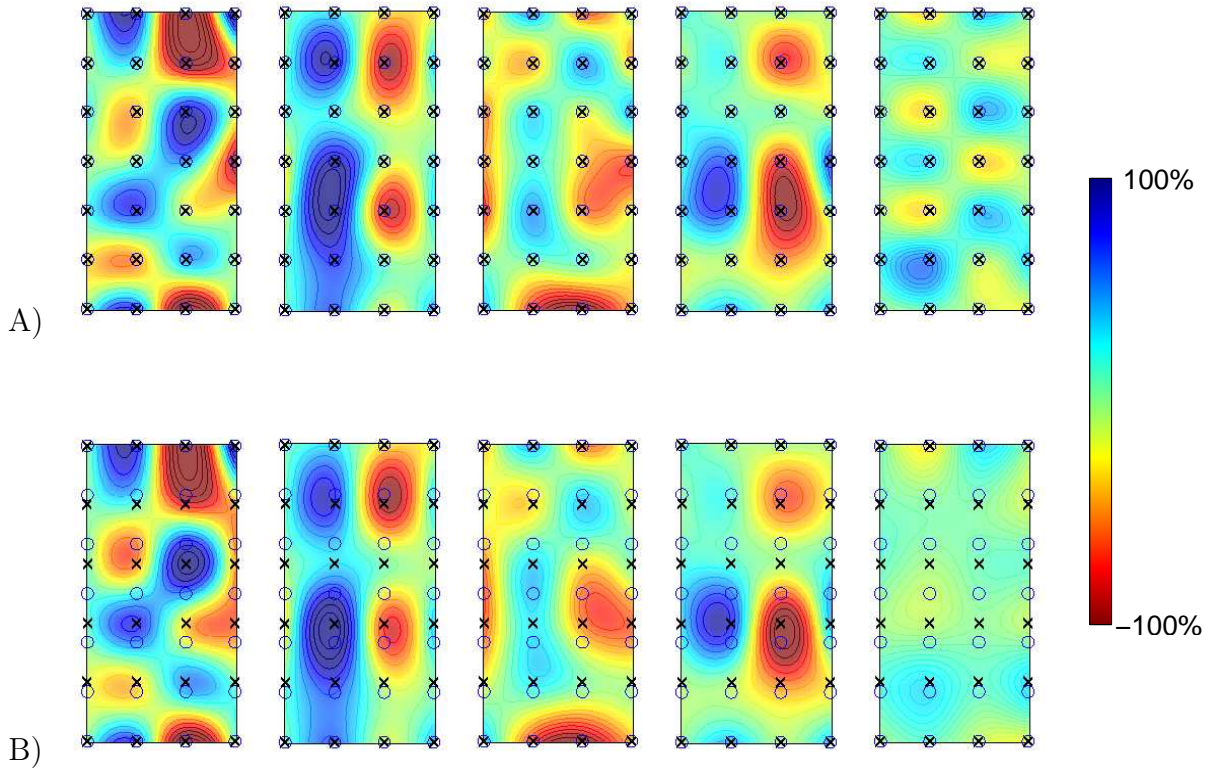


Figure 5: Reconstructions of CSD from experimental data, $t = 15\text{ms}$ after stimulation of vibrissa. For description see caption of Fig. 3.

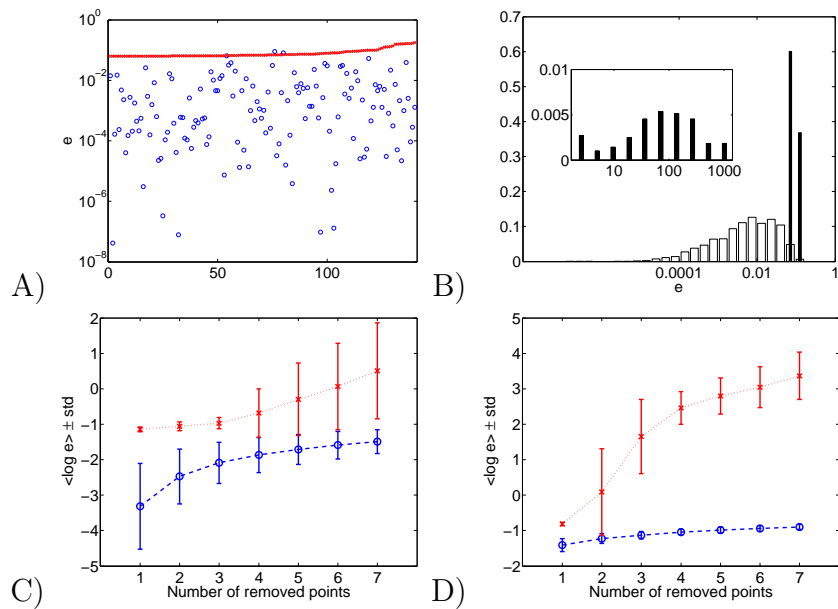


Figure 6: Comparison of LA and LS methods of reconstructing CSD from incomplete data, see caption of Figure 2. The data used here are the same as in Figure 5.

5 Discussion

Reconstruction of the current source density generating recorded extracellular potentials from these potentials is an ill-defined problem. The reason is that there is an infinite number of different distributions which could lead to the same recordings. Nevertheless, as the CSD is much more local reflection of the neural activity than the potentials, there were many attempts to find a viable reconstruction of the sources from the measured fields (Nicholson & Freeman 1975, Mitzdorf 1985, Pettersen et al. 2006). One recent candidate which has a number of advantages over the classical approach is the inverse CSD method (Pettersen et al. 2006, Łęski et al. 2007). It has been originally developed for situations where a set of recordings was collected on a regular rectangular grid. Given the construction of the method it is unclear how to proceed when one of the recordings is missing, due to a failure of one of the electrode contacts or in other cases. We have discussed here two approaches which might enable the application of iCSD method to sets with incomplete data.

Local Averages method (LA) is simple, stable, and the results are never very bad (normalized error of the order of a few percent), even for a relatively large number of missing data points. The Least Squares method (LS) seems attractive as it does not assume anything about the missing data. The distribution of errors is usually bimodal with two narrow modes. Usually, the errors are within a small range dominated by the effect of the sparser grid, however, for a subset of cases which is growing with the number of missing data, the errors can be extremely large.

The respective quality of reconstruction for the two methods depends on the structure of the original sources, and (especially for LS) on the specific location of the removed points. Our tests on the sources modeling the dipole distributions of the cortex (Section 3) with the grid shrinking along the dipole show that for a small number of missing recording points (<5) the LS method usually gives smaller errors than the LA. However, for more complex thalamic sources (Section 4) the LA method is usually far better for any number of removed points.

A priori it is not obvious which method to choose in analysis of experimental data, when the original CSD is unknown and is to be found. Our recommendation is to use the LA method in all cases. Despite its simplicity it seems to be more stable and leads to smaller errors, especially for complex distributions, thus it becomes our method of choice. If the potential seems to vary relatively slowly along one direction of the grid and the missing data are not nearest neighbors lying at the edge, the LS method might also be worth trying, but in general we do not recommend it.

One may wonder if it is possible to improve the technique beyond the proposed approaches. One way would be to consider CSD distributions spanned on the available recording points which would not necessarily form a full regular grid. However, this seems rather difficult to implement in full generality, as the spline coefficients would have to be calculated from the scratch for every distribution of the recording points, and the matrix connecting the potentials with the CSD parameters would have to be calculated for every distribution adding substantially to the computational overhead. A more promising approach seems through the application of statistical methods. For example, one way we plan to follow in the future is to use an overdetermined basis of Gaussian sources and search for efficient projections of the recordings on this basis.

Appendix: Gaussian test sources

The Gaussian sources used in the test in Section 3 were of the form

$$C(x, y, z) = \sum_{i=1}^8 A_i \exp \left[-\frac{(x - x_i)^2}{2(\sigma_i^{xz})^2} - \frac{(y - y_i)^2}{2(\sigma_i^y)^2} - \frac{(z - z_i)^2}{2(\sigma_i^{xz})^2} \right],$$

with the coefficients given in Table 1. Fig. 1 shows four parallel sections of the sources

i	1	2	3	4	5	6	7	8
x_i	1	4	1	4	1	4	1	4
y_i	1	1	4	4	1	1	4	4
z_i	3.5	3.5	3.5	3.5	6.5	6.5	6.5	6.5
σ_i^{xz}	1	1	1	1	1	1	1	1
σ_i^y	1.5	1.5	1.5	1.5	1	1	1	1
A_i	0.8	-1.1	-1.2	1	-1	1.2	0.5	-0.9

Table 1: Coefficients of the Gaussian sources. Origin of the grid is $(x, y, z) = (1, 1, 1)$.

which together pass through all the nodes of the grid (in the region spanned by the virtual recording grid). To calculate the potentials we truncated the sources to the region $-1 \leq x \leq 6$, $-1 \leq y \leq 12$, $-1 \leq z \leq 6$.

Acknowledgements

This work was partly financed from the Polish Ministry of Science and Higher Education research grants N401 146 31/3239 and PBZ/MNiSW/07/2006/11. SŁ was supported by the Foundation for Polish Science.

References

- Barthó, P., Hirase, H., Monconduit, L., Zugaro, M., Harris, K. D. & Buzsáki, G. (2004), ‘Characterization of neocortical principal cells and interneurons by network interactions and extracellular features.’, *J Neurophysiol* **92**(1), 600–608.
- Buzsáki, G. (2004), ‘Large-scale recording of neuronal ensembles.’, *Nat Neurosci* **7**(5), 446–451.
- Csicsvari, J., Henze, D. A., Jamieson, B., Harris, K. D., Sirota, A., Barthó, P., Wise, K. D. & Buzsáki, G. (2003), ‘Massively parallel recording of unit and local field potentials with silicon-based electrodes.’, *J Neurophysiol* **90**(2), 1314–1323.
- de Solages, C., Szapiro, G., Brunel, N., Hakim, V., Isope, P., Buisseret, P., Rousseau, C., Barbour, B. & Léna, C. (2008), ‘High-frequency organization and synchrony of activity in the purkinje cell layer of the cerebellum.’, *Neuron* **58**(5), 775–788.
- Freeman, J. A. & Nicholson, C. (1975), ‘Experimental optimization of current source-density technique for anuran cerebellum.’, *J Neurophysiol* **38**(2), 369–382.

- Holsheimer, J. (1987), 'Electrical conductivity of the hippocampal ca1 layers and application to current-source-density analysis.', *Exp Brain Res* **67**(2), 402–410.
- Ibarz, J. M., Makarova, I. & Herreras, O. (2006), 'Relation of apical dendritic spikes to output decision in ca1 pyramidal cells during synchronous activation: a computational study.', *Eur J Neurosci* **23**(5), 1219–1233.
- Lakatos, P., Shah, A. S., Knuth, K. H., Ulbert, I., Karmos, G. & Schroeder, C. E. (2005), 'An oscillatory hierarchy controlling neuronal excitability and stimulus processing in the auditory cortex.', *J Neurophysiol* **94**(3), 1904–1911.
- Lipton, M. L., Fu, K.-M. G., Branch, C. A. & Schroeder, C. E. (2006), 'Ipsilateral hand input to area 3b revealed by converging hemodynamic and electrophysiological analyses in macaque monkeys.', *J Neurosci* **26**(1), 180–185.
- Logothetis, N. K., Kayser, C. & OeltermannP, A. (2007), 'In vivo measurement of cortical impedance spectrum in monkeys: implications for signal propagation.', *Neuron* **55**(5), 809–823.
- Łeski, S., Wójcik, D. K., Tereszczuk, J., Świejkowski, D. A., Kublik, E. & Wróbel, A. (2007), 'Inverse current-source density method in 3D: reconstruction fidelity, boundary effects, and influence of distant sources.', *Neuroinformatics* **5**(4), 207–222.
- Łeski, S., Pettersen, K. H., Einevoll, G. T., Gigg, J., Kublik, E., Świejkowski, D. A., Tunstall, B., Wróbel, A. & Wójcik, D. K. (2008), 'The Inverse Current Source Density (iCSD) method: Precise estimation of CSD from multi-electrode recordings with one, two and three dimensional contact grids.', presentation at INCF booth, Society for Neuroscience Annual Meeting 2008, Washington
- Makarova, J., Gómez-Galán, M. & Herreras, O. (2008), 'Variations in tissue resistivity and in the extension of activated neuron domains shape the voltage signal during spreading depression in the ca1 in vivo.', *Eur J Neurosci* **27**(2), 444–456.
- Mitzdorf, U. (1985), 'Current source-density method and application in cat cerebral cortex: investigation of evoked potentials and EEG phenomena.', *Physiol Rev* **65**(1), 37–100.
- Nicholson, C. & Freeman, J. A. (1975), 'Theory of current source-density analysis and determination of conductivity tensor for anuran cerebellum.', *J Neurophysiol* **38**(2), 356–368.
- Nunez, P. L. & Srinivasan, R. (2005), *Electric Fields of the Brain: The Neurophysics of EEG*, Oxford University Press.
- Pettersen, K. H., Devor, A., Ulbert, I., Dale, A. M. & Einevoll, G. T. (2006), 'Current-source density estimation based on inversion of electrostatic forward solution: effects of finite extent of neuronal activity and conductivity discontinuities.', *J Neurosci Methods* **154**(1-2), 116–133.
- Pettersen, K. H., Hagen, E. & Einevoll, G. T. (2008), 'Estimation of population firing rates and current source densities from laminar electrode recordings.', *J Comput Neurosci* **24**(3), 291–313.
- Plonsey, R. (1969), *Bioelectric phenomena*, McGraw-Hill Book Company, New York.

- Rajkai, C., Lakatos, P., Chen, C.-M., Pincze, Z., Karmos, G. & Schroeder, C. E. (2008), ‘Transient cortical excitation at the onset of visual fixation.’, *Cereb Cortex* **18**(1), 200–209.
- Schroeder, C. E., Tenke, C. E. & Givre, S. J. (1992), ‘Subcortical contributions to the surface-recorded flash-vep in the awake macaque.’, *Electroencephalogr Clin Neurophysiol* **84**(3), 219–231.
- Shimono, K., Brucher, F., Granger, R., Lynch, G. & Taketani, M. (2000), ‘Origins and distribution of cholinergically induced beta rhythms in hippocampal slices.’, *J Neurosci* **20**(22), 8462–8473.
- Tenke, C. E., Schroeder, C. E., Arezzo, J. C. & Vaughan Jr., H. G. (2006), ‘Interpretation of high-resolution current source density profiles: a simulation of sublaminar contributions to the visual evoked potential.’, *Exp Brain Res* **94**(2), 183–192.
- Ylinen, A., Bragin, A., Nádasdy, Z., Jand, G., Szabó, I., Sik, A. & Buzsáki, G. (1995), ‘Sharp wave-associated high-frequency oscillation (200 Hz) in the intact hippocampus: network and intracellular mechanisms.’, *J Neurosci* **15**(1 Pt 1), 30–46.